ARTICLE NO. 79-0668R

C80-017

Airframe Noise Component Interaction Studies

00023
20001

Martin R. Fink* and Robert H. Schlinker†
United Technologies Research Center, East Hartford, Conn.

Acoustic wind-tunnel tests were conducted to examine the noise-generating processes of an airframe during approach flight. The airframe model was a two-dimensional wing section, to which high-lift leading and trailing edge devices and landing gear were added. Far-field conventional microphones were utilized to determine component spectrum levels. An acoustic mirror directional microphone was utilized to examine differences in noise source distributions on airframe components extended separately and in combination. Measured spectra are compared with predictions inferred from aircraft flyover data. Aeroacoustic mechanisms for each airframe component are identified. Component interaction effects on total radiated noise generally were small (within about 2 dB). However, some interactions altered local flow velocities and turbulence levels, causing redistribution of local acoustic source strength. Possibilities for noise reduction exist if trailing edge flaps could be modified to decrease their noise radiation caused by incident turbulent flow.

Introduction

AIRFRAME noise, generated by motion of aircraft external surfaces through the atmosphere, imposes a limit on aircraft minimum noise levels. As propulsion-system noise is reduced by changes to the engines and more extensive use of inlet and exhaust duct acoustic suppression, airframe noise becomes relatively more important. This is most apparent during approach, when engines are operated at relatively low power settings and airframe noise-generating components such as landing gear and wing flaps are deployed.

Several methods are available for predicting airframe noise for approach configurations. Both the drag element method[1] and the noise component method[2] assume that noise radiated by each individual component of the airframe can be calculated independent of the presence of other components. Only the data analysis method[3] implicitly includes component interactions by using analytical models with constraints matched to measured flyover data for one specific aircraft in different configurations. However, acoustic wind-tunnel tests[4] showed that noise radiation from an airframe model with several deployed components differed, over some portions of the frequency range, from the sum of spectra measured by deploying each component separately. Those tests were conducted at relatively low Reynolds numbers (less than 10^6), so these component interaction effects might have been caused by flow processes not typical of those on full-scale airframes.

If noise-reducing interactions can be produced by flow processes which occur at full scale, use of such processes would provide a technique for aircraft noise reduction. Any geometries which result in adverse interactions on noise should be identified so that they can be avoided. The objectives of the present investigation were to 1) measure the noise radiation from individual deployed airframe components, 2) assess the adequacy of existing prediction schemes for calculating those noise levels, 3) measure the noise radiation from airframe components deployed together and compare them with the acoustic sum of data from individual components, and 4) identify aerodynamic changes responsible for the measured component interaction noise effects to indicate how airframe noise could be reduced. This paper summarizes the detailed comparisons.[5]

Presented as Paper 79-0668 at the AIAA 5th Aeroacoustics Conference, Seattle, Wash., March 12-14, 1979; submitted April 12, 1979; revision received Aug. 9, 1979.

Index categories: Noise; Aeroacoustics.

*Senior Consulting Engineer, Aerodynamics. Associate Fellow AIAA.

†Senior Research Engineer, Aeroacoustics & Experimental Gas Dynamics Group. Member AIAA.

Description of Experiment

Wind Tunnel and Instrumentation

The UTRC acoustic wind tunnel[6] has an open-jet test section contained within an anechoic chamber. Maximum airspeed is in excess of 200 m/s (660 fps) for the 53×79-cm (21×31-in.) rectangular cross-section jet used in this test program. The wind-tunnel nozzle was installed with the larger dimension horizontal, and with horizontal side-plates extending downstream from the nozzle.

A top view of the acoustic wind-tunnel test configuration and microphone installation is shown in Fig. 1. The wing model was mounted with its spanwise direction vertical and its pitching axis passing through the nozzle centerline. A directional microphone, consisting of a reflecting surface and focal point microphone, was traversed along a track parallel to the nozzle centerline. The reflector has a 1.067-m (42-in.) aperture spherical surface with 1.346-m (53-in.) radius of curvature. Calibration of the directional microphone system, including scattering of sound by the test section shear layer, has been previously discussed.[7] Resolution half-width (distance for a 3-dB decrease of signal amplitude) was 2.2 cm at 20 kHz frequency. The reflector could be aimed at different spanwise stations by tilting it about a horizontal axis.

Five conventional 0.635-cm (¼-in.) microphones were mounted behind or to the side of the traverse track. These positions did not interfere with the directional microphone motion. Also, preliminary calibrations verified that the microphones were sufficiently far from the chamber wedges to be in the acoustic free field. The only data presented herein are for the 90-deg microphone at 3.25-m (10.66-ft) radius. For frequencies above 1 kHz, all microphones were at least 10 wavelengths from the model and were in the geometric and acoustic far field. Spectra were corrected for atmospheric absorption[8] at ⅓ octave center frequencies from 10 to 40 kHz.

During this test program, measured spectra with conventional microphones contained a broadband hump at high frequencies. Amplitude of this noise increased as direction angle from upstream was increased. The noise was found to radiate from the diffuser inlet lip closest to the microphones.

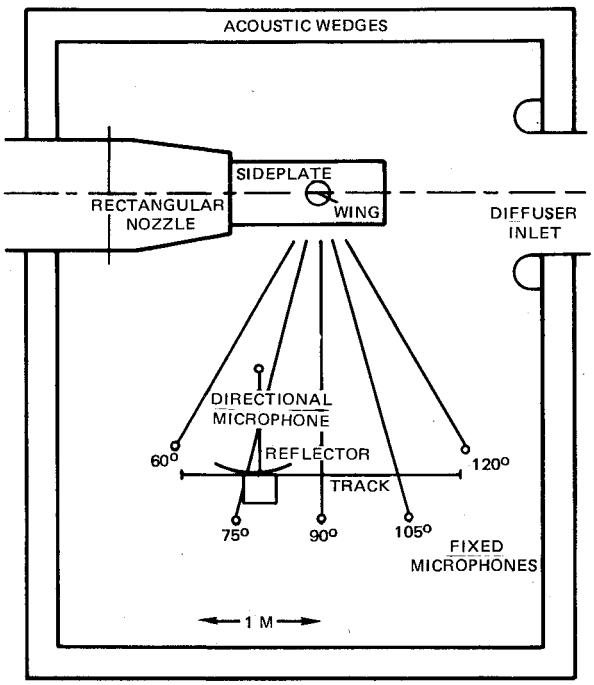

Fig. 1 Top view of United Technologies Research Center (UTRC) acoustic wind-tunnel anechoic chamber and microphone arrangement.

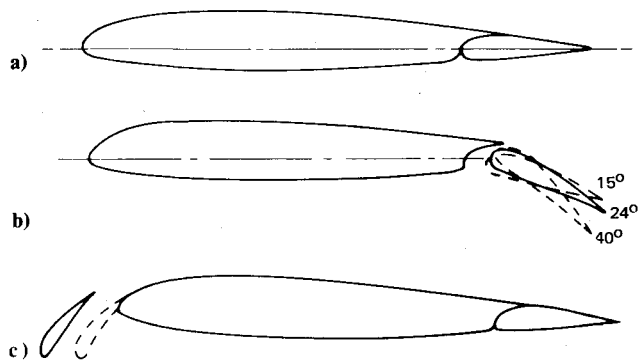

Fig. 2 Airfoil shape of 30.5-cm chord wing with high-lift devices. a) Wing and 25% chord single-slotted trailing edge flap in retracted position. b) Wing and 25% chord single-slotted trailing edge flap at 15-, 24-, and 40-deg deflections. Full and 1/3 span flaps. c) Wing and 15% chord, 25-deg deflection slat installed as either a leading edge flap or leading edge slat, 1/3 span.

It was caused by the deflected airstream, at large lift coefficients, impinging on that rounded surface. A shield of acoustic wedges was installed between the inlet lip and the 90-deg microphone to obstruct and absorb most of this lift-induced background noise.

Airframe Component Model

Clean Wing

An important consideration for this test program was that the test Reynolds number be large enough to achieve aerodynamic flow processes typical of those at full scale. This requirement dictated using the largest practical wing chord, while avoiding excessive flow distortion produced by the lifting wing in the open jet. The latter condition limited the airfoil chord with extended flaps to less than half the open jet height. The resulting basic wing model was chosen to have 0.305-m (1.00-ft) wing chord with all high-lift devices retracted. It was built as an unswept constant chord airfoil model of 53.3-cm (21.0-in.) span. Tests at a typical full-scale approach velocity of 100 m/s (328 fps) correspond to a Reynolds number of about 2×10^6 based on wing chord. Therefore, it was necessary to choose an airfoil section known to have good aerodynamic performance when tested with high-lift devices at this relatively low Reynolds number. Aerodynamic performance of the NACA 23012 airfoil at Reynolds numbers near 2×10^6 with various high-lift devices is known[9,10] to be only slightly below the documented performance at typical full-scale Reynolds numbers. This airfoil shape, rather than a more modern airfoil, was therefore chosen.

Trailing Edge Flaps

The 25% chord single-slotted trailing edge flap employed contour 2-*i*, developed[9] for use with the NACA 23012 airfoil section. As shown in Fig. 2a, the retracted position of this flap produced a closed slot except for the portion of the lower surface near the slot entry. Data were available[10] for this flap shape at a test Reynolds number of 2.2×10^6. Contours of maximum lift coefficient as a function of flap leading edge position had been presented[9] for this flap geometry at various deflections. The resulting trajectory of optimum flap leading edge position as a function of flap angle was utilized to choose the flap positions sketched in Fig. 2b for 15- and 40-deg flap deflection. Maximum lift coefficient occurred approximately at 40-deg deflection angle. Noise amplitudes calculated by the noise component method[2] for these two angles differed by approximately 8 dB. The three spanwise segments could be deployed over the entire 53.5-cm (21.0-in.) span or only the central 1/3 span of 17.8 cm (7.0 in.).

Leading Edge Slat and Flap

Leading edge slat shapes that had been tested with an NACA 23012 airfoil section[11] were representative of aircraft designed only for low subsonic flight speeds. A more practical shape for high-speed cruise was obtained by using the forward lower chord of a leading edge slat developed[12] for an NACA 6-series airfoil. The slat lower surface contour was empirically faired downstream of the 1/3 slat chord (5% airfoil chord) station. An arbitrary 25-deg slat deflection, and optimum slat position for maximum lift coefficient, was used in these tests. This leading edge slat was tested at constant deflection with both the optimum gap and zero gap. At zero gap it represented a leading edge Kreuger flap. These two positions of the leading edge slat are shown in Fig. 2c. This leading edge high-lift device extended only over the central 1/3 span.

Landing Gear

Design of the two-wheel landing gear was based on relative properties of the nose and main landing gear for the Boeing 727 and Douglas DC-9. Wheel diameter was chosen to maintain a large enough Reynolds number to ensure that the measured spectra would be representative of full-scale data. Based on comparisons[13] between model tests and flyover data for full-scale aircraft, the Reynolds number must be at least 2.4×10^5 based on wheel diameter. This was achieved at the lowest test airspeed of 70.7 m/s by use of a 5-cm (2-in.) wheel diameter.

The model comprised two wheels, an axle, a vertical strut, a diagonal brace between the strut and cavity, a door, a door brace, and a rectangular cavity. Spanwise extent of the cavity was large enough to permit mounting the strut at either the midspan or 1/3 span station on the wing. A filler block, contoured to the airfoil lower surface shape, allowed the wing to be tested without the landing gear and cavity.

Test Conditions and Procedures

Airframe noise generally is important only on approach to landing, when all high-lift airframe components are deployed and engine thrust levels are reduced. The lift coefficient of each test configuration was chosen as that which would be used by a full-scale airframe operating with the same

geometry at approach. Approach is generally flown at 1.3 times stalling speed to provide a safety margin for gusts and control motion. For a given altitude and wing loading, flight speed in steady level flight varies inversely with the square root of lift coefficient. Thus, lift coefficient during approach is $(1/1.3)^2$, or 0.6 times maximum lift coefficient. Lift coefficient in these tests therefore was increased as trailing edge flaps were deployed to larger angles and leading edge high-lift devices were added. Resulting approach lift coefficient was predicted to vary from 0.9 to 1.8 over the full range of configurations. The angle of attack at approach lift coefficient was estimated from available aerodynamic data.[9-12] Model angle of attack was increased sufficiently to compensate for the calculated open-jet correction.[5] That is, angle of attack and lift coefficient corrected for open-jet wind-tunnel effects were equal to those for free-air approach conditions.

Tests were conducted at 70.7, 100, and 141.4 m/s (232, 328, and 463 ft/s) wind-tunnel velocities for most configurations. These velocities bracket the flyover velocities of nearly all flight test measurements of airframe noise from turbojet and turbofan aircraft. All effects of flight Mach number on noise amplitude and spectrum shape would then be reproduced. The three airspeeds provided Reynolds numbers of about 1.5×10^6, 2.1×10^6, and 2.9×10^6 based on wing chord, and Mach numbers of about 0.21, 0.30, and 0.42.

Shear Layer Refraction

Sound waves generated at the model are convected downstream within the acoustic wind-tunnel airstream and refracted at the shear layer before reaching the far-field microphones within the anechoic chamber. Resulting effects on measured directivity and SPL amplitude can be significant at these test Mach numbers.

An exaggerated ray path geometry associated with these corrections is sketched in Fig. 3. For a subsonic flow Mach number M, sound waves which travel from the source to the observer are convected within the flow at angle θ_c from the upstream direction. This ray path reaches the shear layer at point A. Nearly all the incident acoustic pressure fluctuation is transmitted across the shear layer. The ray path is refracted to a transmitted angle θ_t smaller than the radiation angle within the flow. Measurements therefore must be corrected[14,15] to the radiation angle θ_c of the ray path within the flow. Resulting corrected data correspond to that from a microphone moving through still air along with the noise source.

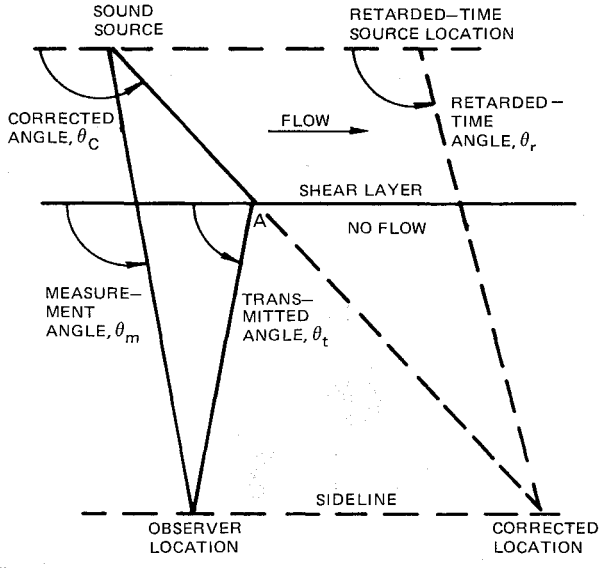

Fig. 3 Sketch of acoustic ray paths as affected by shear layer refraction and frame-of-reference considerations.

For the ease in comparison with theoretical predictions, it is convenient to use a retarded-time coordinate system. This coordinate transformation, plus a Doppler shift, changes the frame of reference to that for a noise source moving relative to the microphone and the air. It effectively moves the noise source downstream relative to its physical location, decreasing the corrected angles to values not very different from the original measured angles. The ray path direction in retarded time, θ_r, is given by

$$\cos\theta_r = \cos\theta_c \sqrt{1 - M^2 \sin^2\theta_c} + M \sin^2\theta_c$$

and the associated change in sound pressure level (SPL) caused by shifting to a constant radius relative to the retarded source position is

$$\Delta\text{SPL} = 20 \log_{10} (\sin\theta_c / \sin\theta_r)$$

For the 90-deg measurement position, data were shifted less than 2 deg in angle and 0.1 dB in amplitude between measured quantities and those for a retarded-time frame of reference.

Airframe flyover data are often presented[3] in a retarded time frame of reference which is fixed relative to the ambient air. If spectra measured in an acoustic wind tunnel are corrected in amplitude by the above procedure and then Doppler-shifted in frequency, they should agree with those flyover data.

Single Component Acoustic Data

Clean Wing

The clean wing with retracted flap was tested at two angles of attack. These corresponded to the airfoil design lift coefficient of 0.30 and an approach lift coefficient of 0.90 for this airfoil without high-lift devices. At the lower lift coefficient, far-field spectra measured with omnidirectional microphones were essentially identical to the background noise of the empty test section. Increased lift coefficient caused an increase of measured SPL at high frequencies. However, this additional noise is believed to be increased background noise of the wind tunnel caused by curvature and deflection of the open jet due to wing lift.

Directional microphone measurements showed the same peak amplitudes for both lift coefficients. These peaks were displaced downstream of the trailing edge by approximately the distance that a sound wave moving perpendicular to the flow would be convected before it reached the shear layer. This result is consistent with a noise mechanism assumed[2] for clean wings: trailing edge noise caused by flow of the wing turbulent boundary layer over the wing trailing edge. Previous directional microphone data for NACA 0012 and 0018 airfoils[7] had demonstrated the same result. This lack of variation in noise over the range from minimum drag to high lift (and therefore high drag) does not agree with predictions by the drag element method.[1]

Absolute-level SPL spectra were calculated by assuming the wing trailing edge to be a line source. Spectra obtained in this manner were as much as 5 dB below the predicted[2] curve. Overprediction had been found in other tests[7] at comparable Reynolds numbers. It had been attributed to the differences in boundary-layer turbulence spectrum shape and level between model and full-scale Reynolds numbers.

Leading Edge Slat and Flap

The leading edge slat was tested only at 70.7- and 100-m/s velocities to avoid large airloads that could overstress its support struts. As with OASPL measured in flyover tests[3] with the DC-9 aircraft over a larger range of airspeeds, the spectra were coalesced by the assumed variation of amplitude with velocity to the fifth power.

The predicted[2] normalized spectrum, based on flyover data for the Vickers VC 10 aircraft[16] with and without its slat

extended, was 4 to 5 dB below the data for these wind-tunnel tests for all but the lowest frequencies. Noise radiation from this model slat is high compared with that of a full-scale slat, possibly due to additional noise from the support struts.

Directional microphone measurements indicated that noise source distributions for the leading edge slat were maximum at the slat trailing edge, which was located approximately at the wing leading edge. Amplitude per unit span was the same at midspan and the slat side edges. Trailing edge noise of the wing was increased, but this noise remained 10 to 15 dB below noise from the slat. Oil flow visualization showed that the airflow was attached to all surfaces except the slat lower surface. The measured slat noise apparently was generated by convection of the slat lower surface separated turbulent flow past the slat trailing edge.

Noise radiation from the leading edge flap, as measured with conventional microphones, was only several dB above tunnel background noise. Measurements with the directional microphone showed that the flap noise came from the region of separated flow at the junction of the flap and wing lower surface. This noise radiation was stronger at the side edges than at midspan. SPLs for this leading edge flap were of the order of 5 dB above the clean wing and 15 dB below the slat.

Landing Gear

The 1/3 octave spectra measured at the 90-deg microphone, with the landing gear and open cavity, were corrected for background noise caused by the lifting wing. They were then normalized in amplitude by adding 20 log $(R/D) - 60$ log $(V/100$ m/s) where D is the wheel diameter. Frequency was normalized as Strouhal number fD/V. Results for the three test velocities were coalesced except for cavity noise, and are about 2 or 3 dB below that predicted by the noise component method[2] adjusted to free field. This prediction is based on a data correlation.[13] They were not changed by moving the gear position from midspan to 1/3 span.

Narrowband analysis of these spectra provided tone frequencies of the cavity in the presence of a landing gear. An equation developed[17] for isolated clean cavities predicted these tone frequencies within 10%, but presence of the landing gear decreased the number of modes excited.

Trailing Edge Flaps

Normalized spectra for the part- and full-span flaps at 15-deg deflection and 90-deg measurement position are compared in Fig. 4. Amplitudes are normalized for flap area and tunnel velocity, and depend only on flap deflection angle. Therefore, the same normalized spectrum is predicted[2] for both part- and full-span flaps. Frequency is normalized as Strouhal number based on flap chord. Data for both the full- and part-span flaps at the three velocities were coalesced by the assumed sixth power velocity variation. Measured levels generally were predicted within about 2 dB for Strouhal numbers larger than 6. Measured spectra were oscillatory, as is predicted[18] for noise radiated by an acoustically non-compact airfoil in turbulent flow.

Normalized spectra measured with the 40-deg deflection part- and full-span trailing edge flaps are compared in Fig. 5.

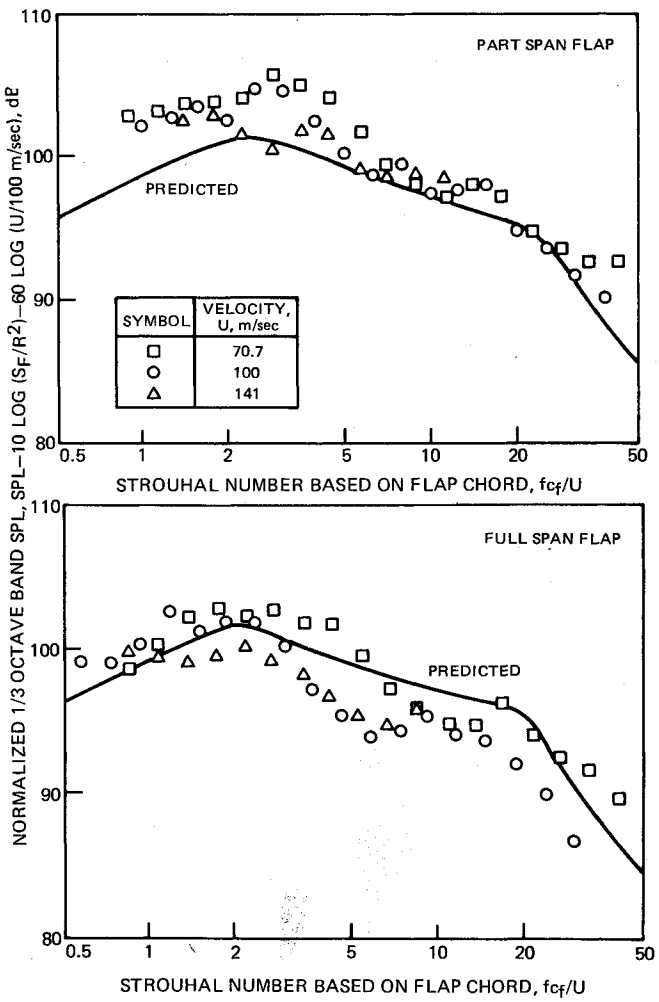

Fig. 4 Comparison of normalized measured and predicted spectra for wing with 15-deg deflection part- and full-span trailing edge flap.

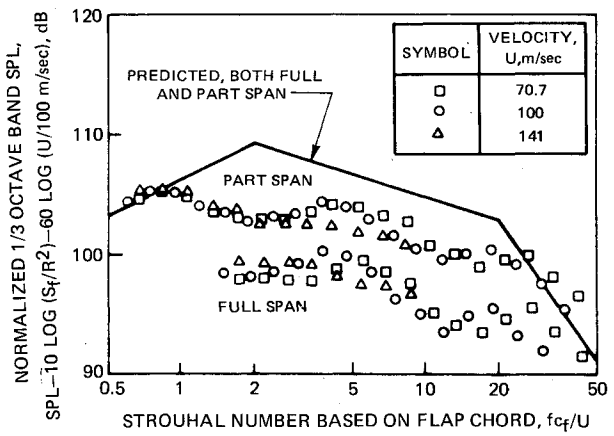

Fig. 5 Comparison of normalized measured and predicted spectra for wing with 40-deg deflection part- and full-span trailing edge flap.

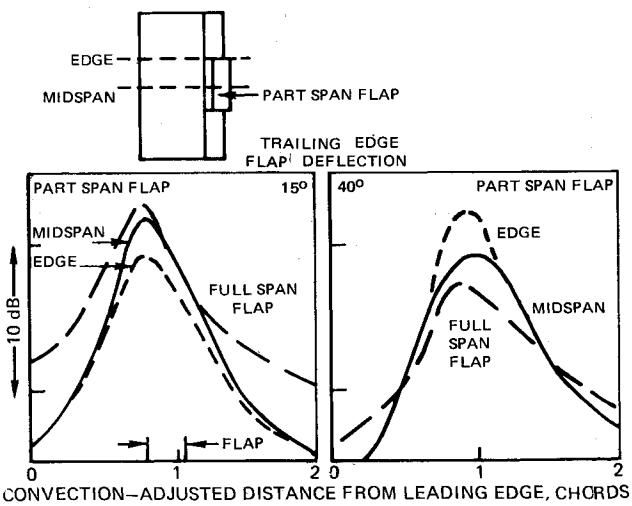

Fig. 6 Chordwise variations of noise source strength at midspan and side edge of part-span trailing edge flap and at midspan of full-span flap, for 15- and 40-deg flap deflections, 100-m/s velocity, 20-kHz model frequency.

Again, the same predicted curve[2] applies for both part- and full-span flaps. However, the normalized data for the full-span flap are 4 to 5 dB below those for the part-span flap. Both configurations radiated about the same amount of noise, even though one had three times the span of the other. The prediction was about 4 dB above data for the part-span flap for Strouhal numbers less than 25.

Streamwise variations of noise source strength at midspan and along a side edge of a part-span single-slotted trailing edge flap are compared in Fig. 6 with those for a full-span flap. Data are shown for 15-deg and 40-deg flap deflection angles at 20-kHz frequency and 100-m/s velocity. Note that the wing is approximately 1/10 to 1/20 of full-scale chord for a jet transport, so these distributions correspond to a frequency of 1 to 2 kHz at full scale. For the smaller angle, apparent source strength increased rapidly as the directional microphone was traversed downstream past the axial position at which sound waves originating at the flap leading edge would reach the far field. Signal strength decayed less rapidly as the microphone was traversed further aft. At this high frequency, the source distribution half-width was larger than the resolution half-width. The flap therefore does not behave as a line source but has its strength distributed along the forward part of the chord.

Noise radiation from midspan was approximately the same for both part-span and full-span flaps at 15-deg deflection. Signal strength from the side edges of the part-span flap was about 3 dB smaller. The full-span flap extended completely across the spanwise region viewed by the reflector, but the part-span flap extended only half way across the viewed region. The observed 3-dB decrease of signal amplitude from midspan to the side edge of the part-span flap therefore corresponds to constant noise source strength per unit span.

Signal strength at midspan of the 40-deg deflection full-span flap had peak amplitude near the convection-adjusted location of the flap leading edge. However, amplitude was about 5 dB below that for the smaller angle. This result is contrary to that predicted by either the drag element[1] or noise component[2] methods. Source distribution for the 40-deg deflection part-span flap was centered near midchord of the flap and was spread along its chord. Noise source strength was stronger at the edge than at midchord. From oil flow visualization, the airflow was attached to the wing and flap surfaces at the smaller deflection. However, at the 40-deg angle, flow separation occurred along roughly the rear half of the flap upper surface. Noise radiation from a highly deflected trailing edge flap therefore is a combination of two flow processes. These are the noise caused by the wing's turbulent wake convected past the flap and the noise caused by convection of the flap upper-surface separated flow past the flap side and trailing edges. Importance of noise radiation from the side edges of trailing edge flaps was first identified by Kendall.[19]

Airframe Component Noise Interactions

Leading Edge Devices and Landing Gear

Leading edge flap, landing gear combinations with the landing gear at either midspan or part-span had much weaker landing gear cavity noise than the landing gear alone. From 5- to 8-dB reduction of the lowest-order tone was achieved. Locally separated flow at the junction of the wing and leading edge flap probably caused a high-turbulence level ahead of the open cavity. The resulting shear layer would be less likely to sustain an aeroacoustic feedback. At higher frequencies, corresponding to full-scale high-annoyance frequencies, SPLs for the two landing gear positions were approximately equal. They were about 1 dB below the acoustic sum of the two individual components.

Unlike the situation for the landing gear and leading edge flap, the slat suppressed the lowest-order cavity tone only for the midspan gear position. Directional microphone traverses for these four combinations show no other interaction effects on source strength.

Leading Edge Flap and Trailing Edge Flaps

The spectrum measured at the 90-deg microphone for 100-m/s velocity with the leading edge flap, 40-deg deflection single-slotted full-span trailing edge flap configuration is plotted in Fig. 7. Also shown are spectra measured for the wing with only the leading edge flap and for the wing with only the trailing edge flap, and their acoustic sum. The acoustic sum is dominated by noise radiation from the trailing edge flap, and spectra for the combination closely match the acoustic sum. Directional microphone traverses validated the lack of interaction effects on trailing edge flap noise.

The spectrum measured with the leading edge flap, 40-deg deflection single-slotted part-span trailing edge flap combination is plotted in Fig. 8. Also shown are spectra measured for the wing with each of the two components, and the acoustic sum of those two spectra. As with the leading edge flap, full-span trailing edge flap combination, the acoustic sum was dominated by the noise spectrum of the trailing edge flap. However, unlike that configuration, the measured spectrum above 6.3-kHz model frequency was about 3 to 4 dB below the acoustic sum of SPLs from the two components. It was 2 to 3 dB below levels measured with the wing and part-span trailing edge flap alone.

Directional microphone traverses at midspan and along the side edge of the part-span high-lift devices are shown in Fig. 9 for 20-kHz center frequency at 100-m/s velocity. The traverses at midspan show increased leading edge flap noise, but slightly decreased trailing edge noise. Thus the noise-reducing interaction did not take place near midspan. Noise radiation from the side edge of the part-span trailing edge flap was reduced by about 4 dB.

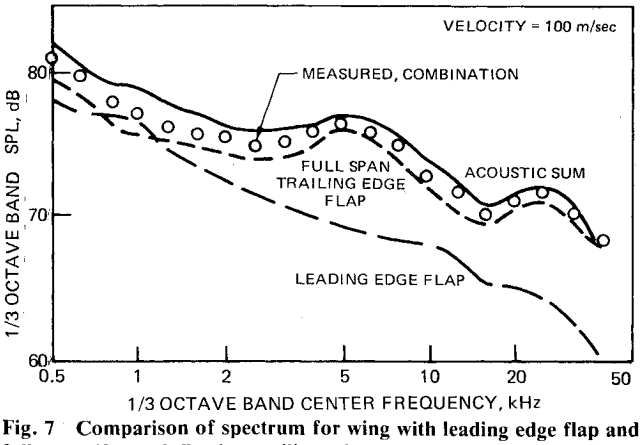

Fig. 7 Comparison of spectrum for wing with leading edge flap and full-span 40-deg deflection trailing edge flap with sum of spectra for wing with each component installed separately.

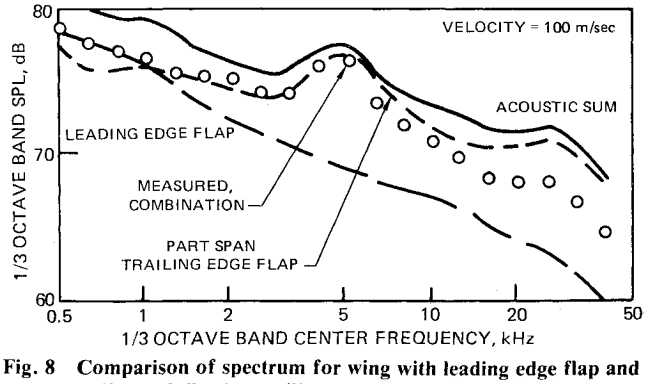

Fig. 8 Comparison of spectrum for wing with leading edge flap and part-span 40-deg deflection trailing edge flap with sum of spectra for wing with each component installed separately.

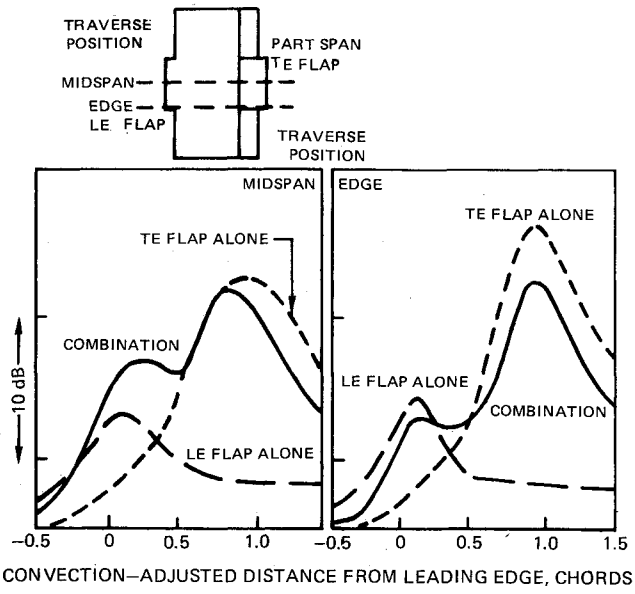

Fig. 9 Chordwise variations of noise source strength for wing with part-span leading and trailing edge flaps and for wing with each component installed separately. 100-m/s velocity, 20-kHz center frequency.

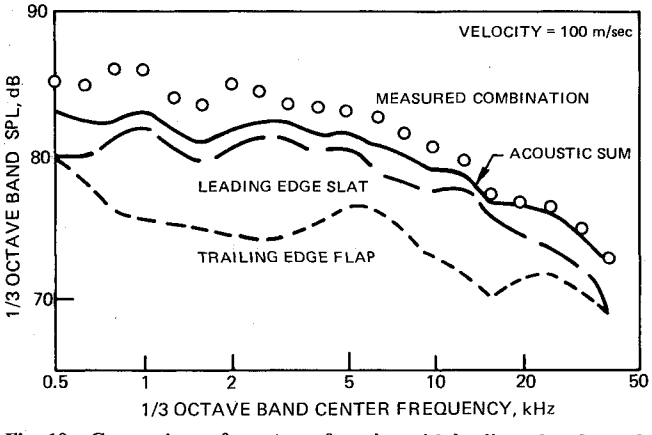

Fig. 10 Comparison of spectrum for wing with leading edge slat and full-span 40-deg deflection trailing edge flap with sum of spectra for wing with each component installed separately.

Peak amplitude of this noise radiation from the flap edge was reduced to about the level which had been measured at midspan with or without the leading edge flap. This was about 1 dB larger than peak amplitude measured on the full-span trailing edge flap. Data for other center frequencies and flow velocities gave similar results. Thus, the favorable component noise interaction shown in the far-field spectra at large Strouhal numbers (Fig. 8) was caused by a decrease of the very strong noise radiation from the side edges of the part-span trailing edge flap.

Leading Edge Slat and Trailing Edge Flaps

Far-field spectra at the 90-deg microphone and 100-m/s velocity for the leading edge slat, full-span trailing edge flap (40-deg deflection angle) combination are plotted in Fig. 10. SPLs for the combination at frequencies up to about 10 kHz were several decibels above the acoustic sum of spectra measured with the slat and flap deflected separately. This sum is dominated by noise radiation from the leading edge slat. At higher frequencies corresponding to the full-scale frequencies which have largest contributions to annoyance, the measured spectra agreed with the acoustic sum of component spectra.

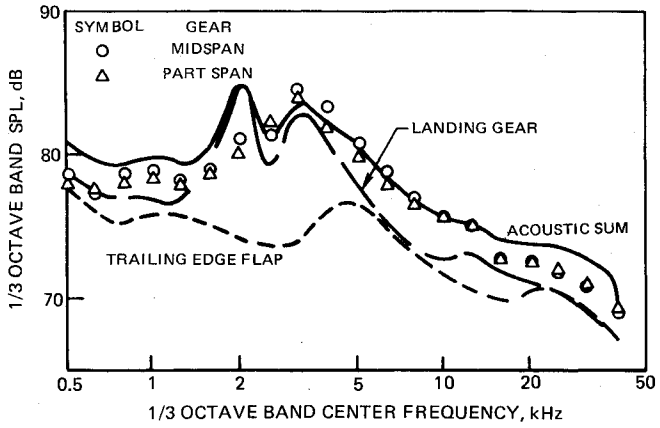

Fig. 11 Comparison of spectra for wing with landing gear and part-span 40-deg deflection trailing edge flap with sum of spectra for wing with each component installed separately.

Noise source strength distributions obtained with the directional microphone showed up to 5-dB decreased noise from the slat side edges, accompanied by 4-dB increased noise from midspan of the trailing edge flap. These redistributions of noise source strength approximately compensated each other. This result is of practical importance because it may be difficult to modify a small-chord, highly loaded slat for noise reduction. Such modifications may be more readily applied to large-chord trailing edge flaps.

Far-field spectra for the leading-edge slat, part-span trailing edge flap combination also showed 2-dB unfavorable interaction below 10-kHz model frequency. For higher frequencies the data were about 1 dB below the acoustic sum. Directional microphone data indicate reduced slat noise and increased flap noise at midspan and relatively little change at the slat and flap side edges.

Noise from the slat edge therefore was decreased by the full-span trailing edge flap, but was only slightly affected by the part-span trailing edge flap. Noise radiation from the midspan region of both part-span and full-span trailing edge flaps was increased by the presence of a leading edge slat. The strong noise radiation from the side edge of a part-span trailing edge flap was unaffected by the upstream presence of a leading edge slat.

Landing Gear and Trailing Edge Flaps

Spectra measured at the 90-deg microphone for the part-span trailing edge flap, open landing gear cavity, landing gear at midspan and part-span configurations at 100 m/s are plotted in Fig. 11. Also shown are measured spectra for the wing with only the part-span trailing edge flap and the wing with only the landing gear and open cavity, and the acoustic sum of those two spectra. Landing gear cavity noise dominated the acoustic sum at the lower frequencies, and both components were important at high frequencies. Below about 12.5-kHz model frequency, SPLs measured for the combination were approximately equal to the sum of the two individual spectra. Above that frequency, the noise radiation for both landing gear positions was about 2 dB less than the acoustic sum.

The directional microphone traces show a redistribution of noise source strength caused by aerodynamic interaction between the landing gear and trailing edge flaps. The deflected flap and increased lift coefficient would be expected to reduce the local velocity near the landing gear, thereby reducing its noise radiation. The landing gear, in turn, would be expected to shed a turbulent wake that impinges upon the trailing edge flap and increases its noise radiation. Aircraft landing gears cannot be easily modified for noise reduction. However, the component interaction found in this study provides reduction of landing gear noise by the trailing edge

flap aerodynamic flowfield. Increased trailing edge flap noise caused by the landing gear turbulent wake might then be reduced by use of acoustically treated flap surfaces.

Approach Configuration

Eight approach configurations were tested, comprising a part-span leading edge slat or flap, extended landing gear at midspan or part-span, and part-span or full-span 40-deg deflection single-slotted trailing edge flaps. Noise-reducing interactions were smaller for these cases than for the favorable two-component interactions. SPLs for the configurations with part-span leading edge flap, part-span trailing edge flap, and either spanwise position of the landing gear were 2 to 3 dB below the acoustic sum of component spectra.

All approach configurations which included a leading edge slat had far-field SPLs within 1 dB of the acoustic sum of component spectra. This result is reasonable because tests of the slat with only one other component gave essentially the same result.

Conclusions

1) Airframe noise component interaction effects on far-field acoustic spectrum are small and generally are within the accuracy of noise prediction for isolated components. However, local noise source strength often was reduced on upstream components and increased on trailing edge flaps. If acoustic impedance of trailing edge flap surfaces and edges could be tailored to reduce their acoustic response to convected turbulence, larger favorable interactions on total noise could be achieved.

2) A part-span leading edge flap in line with a highly deflected part-span trailing edge flap can reduce noise radiation from the trailing edge flap's side edges. This component interaction produced noise levels 3 to 4 dB below the acoustic sum of spectra for the two components deflected individually at high model frequencies, which scale to frequencies having high annoyance.

3) Combinations of a landing gear and a downstream trailing edge flap produced up to 2-dB noise reduction relative to the acoustic sum of component spectra at high model frequencies. This small effect generally occurred as a combination of decreased landing gear noise and a smaller increase of trailing edge flap noise.

Acknowledgment

This work was supported by the NASA Langley Research Center under Contract NAS1-15083.

References

[1] Revell, J.D., Healy, G.J., and Gibson, J.S., "Methods for the Prediction of Airframe Aerodynamic Noise," Aeroacoustics: Acoustic Wake Propagation: Aircraft Noise Prediction: Aeroacoustics Instrumentation, *Progress in Aeronautics and Astronautics*, Vol. 46, M.I.T. Press, Cambridge, Mass., 1976, pp. 139-154. Also AIAA Paper 75-539, AIAA 2nd Aeroacoustics Conference, Hampton, Va., March 24-26, 1975.

[2] Fink, M.R., "Airframe Noise Prediction Method," FAA-RD-77-29, March 1977. Also AIAA Paper 77-1271, AIAA 4th Aeroacoustics Conference, Atlanta, Ga., Oct. 3-5, 1977.

[3] Bauer, A.B. and Munson, A.G., "Airframe Noise of the DC-9-31," NASA CR-3027, July 1978.

[4] Shearin, J.G. and Fratello, D.J., "Airframe Noise of Component Interactions on a Large Transport Model," AIAA Paper 77-57, AIAA 15th Aerospace Sciences Meeting, Los Angeles, Calif. Jan. 24-26, 1977.

[5] Fink, M.R. and Schlinker, R.H., "Airframe Noise Component Interaction Studies," NASA CR 3110, March 1979.

[6] Paterson, R.W., Vogt, P.G., and Foley, W.M., "Design and Development of the United Aircraft Research Laboratories Acoustic Research Tunnel," *Journal of Aircraft*, Vol. 10, July 1973, pp. 427-433.

[7] Schlinker, R.H., "Airfoil Trailing Edge Noise Measurements with a Directional Microphone System," AIAA Paper 77-1269, AIAA 4th Aeroacoustics Conference, Atlanta, Ga., Oct. 3-5, 1977.

[8] Shields, F.D. and Bass, H.E., "Atmospheric Absorption of High Frequency Noise and Application to Fractional-Octave Bands," NASA CR 2760, June 1977.

[9] Wenzinger, C.J. and Harris, T.A., "Wind-Tunnel Investigation of an NACA 23012 Airfoil with Various Arrangements of Slotted Flaps," NACA Report 664, 1939.

[10] Cahill, J.F., "Summary of Section Data on Trailing-Edge High-Lift Devices," NACA Rept. 938, 1949.

[11] Bamber, M.J., "Wind-Tunnel Tests of Several Forms of Fixed Wing Slot in Combination with a Slotted Flap on a NACA 23012 Airfoil," NACA TN 702, April 1939.

[12] Quinn, J.J., Jr., "Tests of the NACA 64_1A212 Airfoil Section with a Slat, a Double Slatted Flap, and Boundary Layer Control by Suction," NACA TN 1293, May 1947.

[13] Heller, H.H. and Dobrzynski, W.M., "Sound Radiation from Aircraft Wheel-Well/Landing Gear Configurations," *Journal of Aircraft*, Vol. 4, Aug. 1977, pp. 768-774.

[14] Amiet, R.K., "Correction of Open-Jet Wind-Tunnel Measurements for Shear Layer Refraction," Aeroacoustics: Acoustic Wave Propagation, Aircraft Noise Prediction: Aeroacoustic Instrumentation, *Progress in Aeronautics and Astronautics*, Vol. 46, M.I.T. Press, Cambridge, Mass. 1976, pp. 259-280. Also AIAA Paper 75-532, AIAA 2nd Aeroacoustics Conference, Hampton, Va., March 24-26, 1975.

[15] Amiet, R.K., "Refraction of Sound by a Shear Layer," *Journal of Sound and Vibration*, Vol. 58, June 1978, pp. 467-482.

[16] Fethney, P., "An Experimental Study of Airframe Self-Noise," Aeroacoustics: STOL Noise: Airframe and Airfoil Noise, *Progress in Aeronautics and Astronautics*, Vol. 45, M.I.T. Press, Cambridge, Mass., 1976, pp. 379-403. Also AIAA Paper 75-511, AIAA 2nd Aeroacoustics Confernce, Hampton, Va., March 24-26, 1975.

[17] Block, P.J.W., "Measurements of the Tonal Component of Cavity Noise and Comparison with Theory," NASA TP 1013, Nov. 1977.

[18] Paterson, R.W. and Amiet, R.K., "Acoustic Radiation and Surface Pressure Characteristics of an Airfoil Due to Incidence Turbulence," NASA CR 2733, Sept. 1976. Also *Journal of Aircraft*, Vol. 14, Aug. 1977, pp. 729-736.

[19] Kendall, J.M., "Measurements of Noise Predicted by Flow Past Lifting Surfaces," AIAA Paper 78-239, AIAA 16th Aerospace Sciences Meeting, Huntsville, Ala., Jan. 16-18, 1978.